

Observations of the temperature dependent response of ozone to NO_x reductions in the Sacramento, CA urban plume

B. W. LaFranchi^{1,*}, A. H. Goldstein^{2,3}, and R. C. Cohen^{1,4}

¹Department of Chemistry, University of California, Berkeley, CA, USA

²Department of Environmental Science, Policy, and Management, University of California, Berkeley, CA, USA

³Department of Civil and Environmental Engineering, University of California, Berkeley, USA

⁴Department of Earth and Planetary Science, University of California, Berkeley, USA

* now at: Center for Accelerator Mass Spectrometry, Lawrence Livermore National Laboratory, Livermore, CA, USA

Received: 12 January 2011 – Published in Atmos. Chem. Phys. Discuss.: 22 February 2011

Revised: 25 May 2011 – Accepted: 29 June 2011 – Published: 18 July 2011

Abstract. Observations of NO_x in the Sacramento, CA region show that mixing ratios decreased by 30 % between 2001 and 2008. Here we use an observation-based method to quantify net ozone (O₃) production rates in the outflow from the Sacramento metropolitan region and examine the O₃ decrease resulting from reductions in NO_x emissions. This observational method does not rely on assumptions about detailed chemistry of ozone production, rather it is an independent means to verify and test these assumptions. We use an instantaneous steady-state model as well as a detailed 1-D plume model to aid in interpretation of the ozone production inferred from observations. In agreement with the models, the observations show that early in the plume, the NO_x dependence for O_x (O_x = O₃ + NO₂) production is strongly coupled with temperature, suggesting that temperature-dependent biogenic VOC emissions and other temperature-related effects can drive O_x production between NO_x-limited and NO_x-suppressed regimes. As a result, NO_x reductions were found to be most effective at higher temperatures over the 7 year period. We show that violations of the California 1-h O₃ standard (90 ppb) in the region have been decreasing linearly with decreases in NO_x (at a given temperature) and predict that reductions of NO_x concentrations (and presumably emissions) by an additional 30 % (relative to 2007 levels) will eliminate violations of the state 1 h standard in the region. If current trends continue, a 30 % decrease in NO_x is expected by 2012, and an end to violations of the 1 h standard in the Sacramento region appears to be imminent.

1 Introduction

Many populated regions worldwide have chronically high levels of summertime ozone produced during the photochemical oxidation of carbon monoxide (CO) and volatile organic compounds (VOCs) in the presence of NO_x (NO_x = NO + NO₂). Protecting human health (Uysal and Schapira, 2003; Trasande and Thurston, 2005; McClellan et al., 2009; Yang and Omaye, 2009) and agriculture (Morgan et al., 2003; Ashmore, 2005; Feng and Kobayashi, 2009; Fuhrer, 2009) has required local regulation aimed at reducing VOC and NO_x levels.

Two informative examples of this are Mexico City (Zavala et al., 2009) and Beijing (Tang et al., 2009), which have been subject to two contrasting emission control strategies. In Mexico City, VOC emissions decreased significantly between 1992 and 2006 while NO_x emissions stayed relatively constant; O₃ concentrations decreased during this time at a rate close to 3 ppb yr⁻¹. In contrast, in Beijing, O₃ concentrations increased over a 5 year period, from 2001 to 2006, in response to controls on NO_x with no corresponding reduction in VOC emissions. The results observed in both cities are in line with what would be predicted, in a qualitative sense, from the chemical mechanisms of O₃ production in a VOC-limited atmosphere, typical of polluted cities.

The contrasting examples of Mexico City and Beijing show that the way in which emission controls are implemented can result in varying levels of success, or in some cases, detriment, in controlling O₃ concentrations. Complicating matters, however, is that the O₃ response to identical control strategies is not always the same in different regions. For example, in Los Angeles, combined VOC and NO_x controls resulted in a nearly 50 % decrease in peak 1 h



Correspondence to: R. C. Cohen
(rccohen@berkeley.edu)

O₃ concentrations from 1990 (310 ppb) to 2007 (159 ppb), however the San Joaquin Valley in Central California, which was subject to essentially the same controls, showed only a marginal decrease in peak 1 h O₃ (164 ppb to 142 ppb) over this time frame (Cox et al., 2009).

While we have an adequate qualitative understanding of the response of O₃ to NO_x and/or VOC reductions, a quantitative analysis remains elusive (e.g. Thornton et al., 2002), presumably because of our incomplete knowledge of the relevant emissions and photochemistry and our inability to represent the meteorology with sufficient accuracy. As it is unclear which aspects of our chemical understanding need improvement, direct tests of the mechanisms by comparison to observations in the ambient atmosphere are needed.

One of the primary difficulties with such an analysis is that controlled experiments where a single parameter is varied while all others are held constant are almost never realized in the atmosphere. Day-of-week effects on ozone are a close approximation to a control experiment, because NO_x emissions typically decrease significantly on weekends with relatively small changes in VOC emissions. Still, in most locations, meteorology varies too much to directly compare weekends and weekdays in a given year, and long term decreases in NO_x and VOCs, along with changes in land use, makes year to year comparisons subject to the difficulties of interpreting an experiment where many things have changed at once.

The Sacramento, California (38.58° N, 121.49° W) urban plume offers a rare opportunity for evaluating effects of changes in a single parameter, NO_x concentrations, on atmospheric chemistry using ambient measurements. The local topography in the region results in an extremely stable wind field, with upslope flow during the daytime, and downslope flow at night, driven by heating and cooling in California's central valley (e.g. Carroll and Dixon, 2002; Dillon et al., 2002). The VOCs that control ozone production in the region are predominantly biogenic (Dreyfus et al., 2002; Cleary et al., 2005; Steiner et al., 2008). Variability in NO_x, therefore, is completely decoupled from variability in VOCs in the region.

NO_x mixing ratios in the Greater Sacramento Area (as we will discuss below) and throughout Northern California (Ban-Weiss et al., 2008; Cox et al., 2009; Russell et al., 2010) have been in steady decline for over a decade, thus facilitating an atmospheric experiment in which only a single variable in the ozone production system has been changed (at a given temperature). Previous work (Murphy et al., 2006b, 2007) has investigated the effect of day-of-week changes in NO_x emissions on O₃ production in the region. Here, with variability in NO_x occurring on both day-of-week and inter-annual time-scales, we are able to compare the effects of NO_x reductions within a single year (weekdays vs. weekends) to the equivalent NO_x reductions on weekdays several years later.

In what follows, we will give a description of the Sacramento urban plume (Sect. 2), highlighting previous efforts to characterize its chemistry. We then describe our observation based method for inferring the production of ozone (P(O₃)) in an urban plume (Sect. 3) and describe the correlations of the inferred P(O₃) with temperature and NO_x (Sect. 4). We will compare our observations to results from a steady-state model and a time-dependent Lagrangian plume model (Sect. 5) and discuss the implications of our results for air quality in the region (Sect. 6).

2 The Sacramento urban plume

Due to its extremely regular, topographically-driven wind patterns, the Sacramento region can be represented as a simple flow reactor with dilution (Carroll and Dixon, 2002; Dillon et al., 2002; Pérez et al., 2009). This Lagrangian representation holds for a significant portion of the year and greatly facilitates the understanding of changes in photochemical conditions over diurnal (Murphy et al., 2006a; Day et al., 2009), weekly (Murphy et al., 2007), seasonal (Murphy et al., 2006a; Day et al., 2008; Farmer and Cohen, 2008), and, as in the present study, inter-annual timescales.

A map of the Greater Sacramento Area (GSA) and the downwind regions influenced by the urban plume is shown in Fig. 1. We will refer to three different sub-regions in this discussion: the urban core, the suburbs, and the foothills. A number of monitoring sites operated by the California Air Resources Board (CARB) are located within the study region, as shown in Fig. 1, as are two UC Berkeley research sites. Exceedances of both the 1 h and 8 h CA standard are yearly occurrences during the so-called ozone season, typically from May to September.

In the GSA, biogenic VOCs are the main source of VOC reactivity that leads to ozone production. In all phases of the plume evolution, biogenic VOC emissions dominate VOC reactivity (Cleary et al., 2005; Steiner et al., 2008). Isoprene emissions are strong in the metropolitan region and peak within a roughly 10 km wide band of oak forest that runs north-south along the western edge of the Sierra Nevada foothills (Dreyfus et al., 2002; Spaulding et al., 2003). Isoprene and its oxidation products represent the majority of VOC reactivity throughout the plume. East of the oak band methyl but-2-ene-3-ol (MBO), and terpenoid species are added to the mix and become a larger fraction of the reactivity (Lamanna and Goldstein, 1999; Schade et al., 2000; Bouvier-Brown et al., 2009).

Early studies of the plume found that ozone concentrations peak some 50 km downwind of the city center and decrease significantly over the next 15 km of travel (Carroll and Dixon, 2002). These authors were among the first to characterize the plume as a Lagrangian air parcel that migrates from the urban core to the sparsely populated Sierra Nevada Mountains. Using a suite of VOC measurements

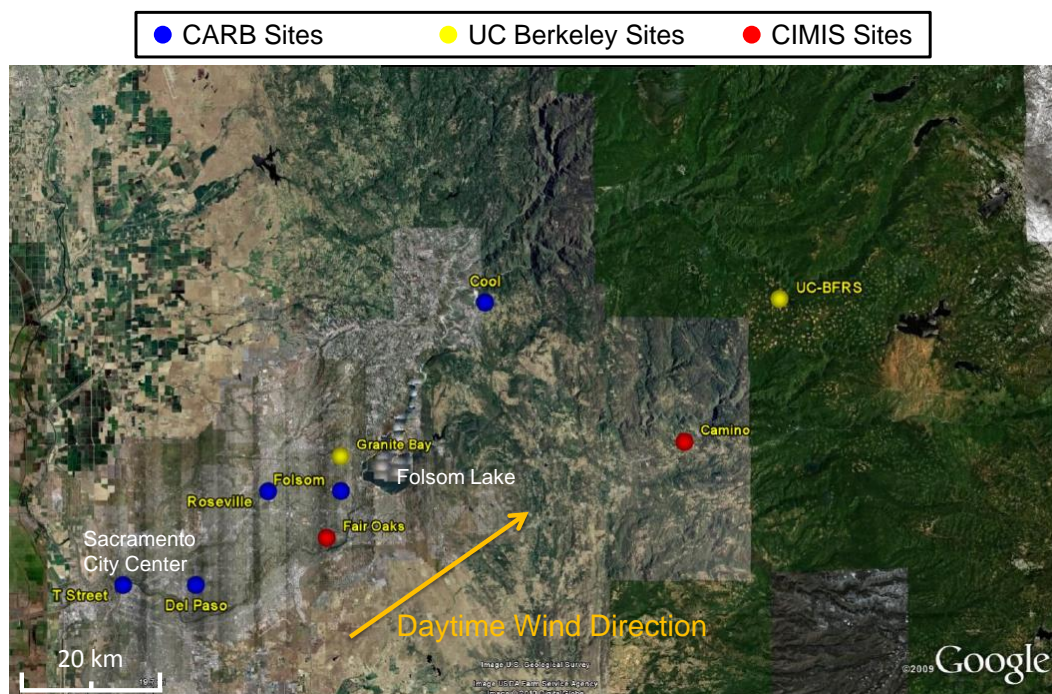


Fig. 1. Map of the Greater Sacramento Area indicating the location of monitoring stations used in this analysis. Yellow circles are UC Berkeley research sites, blue circles are CARB monitoring sites, and red circles are CIMIS weather stations. Map created using Google Earth.

at Granite Bay, in the suburbs to the southwest of Folsom Lake, and downwind at UC Blodgett Forest Research Station (UC-BFRS), Dillon et al. (2002) took advantage of the Lagrangian nature of the plume in order to characterize the average mixing and oxidation characteristics of the plume. More recently, Pérez et al. (2009) built on this conceptual framework for plume transport and incorporated a detailed chemical model in order to test the mechanistic understanding of NO_x chemistry as it pertains to ozone production.

Murphy et al. (2006b, 2007) analyzed the day-of-week patterns of several species related to photochemical ozone production at various points along the plume transect and identified a change in the NO_x dependence for ozone production as the plume migrates downwind. In addition to an analysis of day-of-week differences in NO_x, O₃, and isoprene concentrations, observations of the NO_z/NO_x ratio (NO_z = NO_y – NO_x) at two different locations in the Sacramento urban plume, one at Granite Bay, in the suburbs, and one at UC-BFRS, showed different day-of-week behavior, suggestive of NO_x-suppressed (VOC limited) ozone production in the urban core and suburbs and NO_x-limited ozone production in the foothills. As a result, there was higher observed ozone in the urban core on weekends than on weekdays while the reverse holds at the remote downwind site, during the years 1998–2002 (Murphy et al., 2007).

Our current understanding of the behavior of the Sacramento urban plume is summarized as follows:

- The regular meteorology in the region allows for a simplistic representation of the plume as an air parcel moving in a Lagrangian sense to the northeast.
- Dilution of chemical species in the plume occurs at a predictable rate as the plume migrates away from the urban core and mixes with the regional and global background.
- Anthropogenic emissions of NO_x in the plume exhibit strong weekday/weekend differences and have been decreasing over longer time scales, presumably due to replacement of older vehicles with newer ones that have better emission controls.
- VOC reactivity in the plume, even in the urban core, is controlled primarily by biogenic emissions, which vary with temperature and solar radiation, leading to diurnal, seasonal, and synoptic variability.
- O₃ production is VOC-limited in the urban core and transitions to NO_x-limited as the plume is transported into the foothills and away from NO_x sources.

3 Estimating odd-oxygen production rates from observations

As an urban plume evolves, it is influenced by both chemical and physical processes. The rate of change in concentration

Table 1. Measurement summary.

Site	ARB Number	Location	Measurements	Uncertainty	Detection Limit
T Street	34 305	38.57, -121.49	NO _y ^a	See Sect. 3	
Del Paso	34 295	38.61, -121.37	NO ^b	10 %	0.4 ppb
			NO _y ^a	See Sect. 3	0.4 ppb
			O ₃ ^c	<1 %	0.6 ppb
Roseville	31 822	38.75, -121.26	NO ^b	10 %	0.4 ppb
			NO _y ^a	See Sect. 3	0.4 ppb
			O ₃ ^c	<1 %	0.6 ppb
Folsom	34 311	38.68, -121.16	NO _y ^a	See Sect. 3	0.4 ppb
Cool	9693	38.89, -121.00	O ₃ ^c	<1 %	0.6 ppb
UC-BFRS	N/A	38.90, -120.63	NO ₂ ^d	10 %	10–20 ppt
			O ₃ ^e	<1 %	0.6 ppb

^a Chemiluminescence following catalytic conversion to NO (Model: API 200E). ^b Chemiluminescence (Model: API 200E). ^c UV photometry (Model: API 400A).

^d Laser induced fluorescence (Thornton et al., 2000). ^e UV photometry (Model: Dasabi 1008-RS).

for a given species in the plume, represented by a box moving with the local winds, is given by:

$$\frac{d[X]}{dt} = P + E - D - L - M \quad (1)$$

where P and L are the rates of chemical production and loss, respectively, E is the emission rate, D is the rate of deposition to the surface, and M is the mixing or entrainment rate of the plume with its surroundings.

For a chemically inert tracer ($P = L = 0$) that has negligible emission sources and does not deposit ($E = D = 0$), its concentration is influenced only by the mixing/entrainment rate M , which we represent as follows:

$$M = k_{\text{mix}} ([X] - [X]_{\text{bkg}}) \quad (2)$$

where k_{mix} is an empirically determined constant and $[X]_{\text{bkg}}$ is the concentration of species X in the background or surrounding air.

For reasons that will be described in Sect. 5, we are interested in the rate of change for odd oxygen ($O_x = O_3 + NO_2$). We assume O_x has no direct emission sources ($E = 0$), and its time derivative can be expressed as:

$$\frac{d [O_x]}{dt} = P - L - D - M. \quad (3)$$

If O_x measurements are made at two locations in the plume, Eq. (3) can be rearranged and the derivative evaluated at those two points to solve for the mean net chemical production ($P - L - D$ or $\Delta [O_x]_{\text{chem}}/\Delta t$) between the two locations as follows:

$$\frac{\Delta [O_x]_{\text{chem}}}{\Delta t} = P - L - D = \frac{\Delta [O_x]_{\text{obs}}}{\Delta t} + M. \quad (4)$$

In Eq. (4), $\Delta [O_x]_{\text{obs}}/\Delta t$ is the observable parameter, calculated from the difference in $[O_x]_{\text{obs}}$ at two adjacent locations in the plume and the time it takes for the air mass to travel between the two sites. We then calculate a time-dependent mixing rate using Eq. (5), and solve for $\Delta [O_x]_{\text{chem}}/\Delta t$.

$$M = \frac{\Delta [O_x]_{\text{mix}}}{\Delta t} = \frac{\int_{t_0}^{t_1} k_{\text{mix}} ([O_x](t) - [O_x]_{\text{bkg}}) dt}{\Delta t}. \quad (5)$$

Other than entrainment, the loss pathways for O_x in the plume are deposition, reaction with VOCs, reaction with HO₂, photolysis followed by the reaction of O¹D atom with H₂O, and reaction of OH with NO₂. The lifetime of O_x with respect to chemical losses and deposition in the PBL is on the order of 20–30 h, an order of magnitude longer than the time differences (Δt) used in our analysis. Thus, variability in the O_x removal rates will have little effect on the observational calculation of $\Delta [O_x]_{\text{chem}}/\Delta t$. Variability in production rates, which often reach 10–30 ppb/h in urban areas, corresponding to O_x lifetimes with respect to production of 2–6 hours, dominate the variability in $\Delta [O_x]_{\text{chem}}/\Delta t$. We derive our estimate for O_x losses based on previously published observations of O₃ and NO₂ fluxes over Blodgett Forest (Kurpius and Goldstein, 2003; Farmer and Cohen, 2008) and observations of VOCs at Granite Bay and at Blodgett Forest (Dillon et al., 2002; Cleary et al., 2005).

Seven years of NO_x and O₃ data were compiled from three CARB sites (Del Paso, Roseville, and Cool) (CARB, 2009) and from UC Berkeley measurements at UC-BFRS between 2001 and 2007. Table 1 summarizes the observations used from each site and the methods of detection. These four sites fall roughly along the center line of the plume and split the

Table 2a All Data (Full Year).

Year	# Days	Wind Direction (deg.)		Wind Speed (m s ⁻¹)		[NO _y] (ppbv)		Roseville O ₃		Cool O ₃		Blodgett O ₃	
		Mean	Std. Err.	Mean	Std. Err.	Mean	Std. Err.	Exc. Days	# Days	Exc. Days	# Days	Exc. Days	# Days
<i>Hot</i>													
2001	64	247.5	2.5	3.5	0.1	17.2	1.3	14	64	32	64	17	63
2002	49	263.4	3.5	3.2	0.1	19.2	1.4	15	49	31	49	18	49
2003	66	260.8	2.6	3.0	0.0	17.2	1.3	13	66	26	66	18	66
2004	53	261.8	2.0	3.4	0.0	14.2	0.8	6	53	12	51	13	51
2005	56	263.3	2.4	2.6	0.1	15.2	0.9	16	56	27	56	9	56
2006	58	255.1	2.6	3.2	0.1	14.3	1.0	20	58	30	58	10	38
2007	49	255.9	2.0	3.3	0.1	12.3	0.8	4	49	6	47	1	14
<i>Medium</i>													
2001	58	248.8	2.4	3.5	0.1	14.1	1.1	1	58	7	54	3	56
2002	62	252.3	2.7	3.4	0.1	15.0	1.0	7	62	21	61	4	62
2003	45	251.9	5.0	3.1	0.1	14.9	1.4	1	45	2	45	2	45
2004	55	249.5	4.1	3.5	0.1	13.5	1.0	1	55	2	50	2	55
2005	47	258.9	3.3	3.0	0.1	13.3	1.2	2	47	4	47	1	41
2006	58	253.6	3.3	3.4	0.1	11.8	0.6	0	58	9	55	1	38
2007	56	248.3	3.6	3.4	0.1	9.1	0.5	1	56	2	55	0	15
<i>Cold</i>													
2001	237	220.6	3.3	2.9	0.1	22.9	1.4	0	237	0	56	0	222
2002	251	235.3	2.9	3.0	0.1	23.7	1.3	0	251	5	71	4	248
2003	250	235.8	2.7	2.7	0.1	21.7	1.2	1	250	3	69	0	234
2004	224	236.9	3.6	3.0	0.1	23.0	1.4	0	224	2	62	0	203
2005	259	236.0	2.9	2.7	0.1	20.9	1.1	0	259	0	78	0	132
2006	242	229.8	3.0	2.6	0.1	19.6	1.1	0	242	1	65	1	74
2007	254	238.5	2.9	2.7	0.1	18.0	1.1	0	249	0	75	0	226

transect into three segments that will be referred to as Segments A (Del Paso to Roseville), B (Roseville to Cool), and C (Cool to UC-BFRS). Temperature and solar radiation measurements from the California Irrigation Management Information System site at Fair Oaks, located roughly in between Del Paso and Roseville, and wind speed and wind direction from the Camino CIMIS site located to the southwest of UC-BFRS (CIMIS, 2009). Table 2a summarizes the full 7 year data set.

The method for NO_x detection at the CARB sites is the catalytic conversion of NO₂ to NO, followed by detection of total NO (ambient plus converted) by chemiluminescence. Subtraction of the NO signal detected in ambient air from the NO_x signal gives the response, labeled “NO₂”. There are known positive artifacts to this measurement (Winer et al., 1974; Grosjean and Harrison, 1985; Dunlea et al., 2007; Steinbacher et al., 2007) as a result of the accompanying conversion of peroxy nitrates (PNs), alkyl and multifunctional alkyl nitrates (ANs), and nitric acid (HNO₃) over the molybdenum oxide (MoO) catalytic converter. In this study, we will assume that these higher oxides are detected with 100 % efficiency and refer to observations reported as “NO_x” by CARB, instead, as NO_y.

For the purpose of understanding the role of NO_x in O_x chemistry, we estimate NO_x mixing ratios from the observations of NO_y. To do this we assume that the sum of the higher oxides of nitrogen are present at the monitoring stations in an amount equal to the NO₂ at those stations (a ratio roughly

consistent with observations of NO₂, PNs, ANs and HNO₃ at the Granite Bay site; Cleary et al., 2005, 2007). Thus, we define NO₂ at these sites as 50 % of the reported “NO₂”. Calculations using the observed NO and O₃, assuming standard parameters for the NO-NO₂-O₃-HO_x steady-state relationship, indicate that NO₂ is 65–70 % of the observed “NO₂”. These two scenarios bracket our uncertainty of the true NO₂ at between 50 and 70 % of the observed “NO₂”.

Based on the average daily wind speed, the Lagrangian plume age, relative to an arbitrary start time (t_0), can be approximated for each measurement site along the transect. Selecting Del Paso as the plume start point and a t_0 of 1000 PST, the plume passes over Roseville, Cool, and UC-BFRS at 1200 PST, 1500 PST, and 1700 PST respectively. Daily values for each available measurement were obtained from 2 h averages about these times.

Equation (4) is solved for $\Delta[\text{O}_x]_{\text{chem}}/\Delta t$ for each plume segment using a constant O₃ background of 53 ppb (NO₂ background is negligible for consideration of odd-oxygen) and $k_{\text{mix}} = 0.31 \text{ h}^{-1}$ (see Appendix B for details). Since there are no nitrogen oxide measurements available at the Cool site, we estimate NO_y (and NO_x) based on an exponential decay from Roseville with a lifetime of 2 h and a transit time of 3 h. The resulting NO_x is consistent with observations of NO_x further downwind at UC-BFRS and amounts to NO₂ levels of at most 3 % of O_x at the site.

The analysis is applied to the months of May through September and uses days when wind speeds are between

3 and 4 m s⁻¹ (at the Camino site), wind direction is W or SW (between 200 and 260°, at Camino), and solar radiation is within 10% of a 30 day running mean (at Fair Oaks) to ensure clear sky conditions. About half of the observations from May through September survive this filter. There is no significant correlation of wind speed or wind direction with temperature or NO_y in this data set ($R^2 < 0.04$). The filtered data used in this analysis is summarized in Table 2c.

4 Observed NO_x and temperature influence on P(O_x)

Figure 2 shows the annual average NO_y observed during the summer months (May–September, 2001–2008) from the average of 4 GSA monitoring sites (T Street, Del Paso, Roseville, and Folsom). Observations are shown for all days, weekdays only, and weekends only. NO_y decreased by 30% from 2001–2008 at an approximate rate of 0.6–0.7 ppb yr⁻¹. This long-term decrease is of the same magnitude as the mean observed weekday-weekend difference over the study period (~5 ppb). The day-of-week effect in the Sacramento region has also been observed in the satellite record (Russell et al., 2010) and was found to have a significant effect on ozone production rates, as reported by Murphy et al. (2006b, 2007).

It is our expectation that the primary variables causing changes in ozone production rates are the NO_x and biogenic VOC concentrations. Since BVOCs are emitted as an exponential function of temperature, we use temperature as a surrogate to represent changes in VOC reactivity. Changes in radical propagating reaction rates and water vapor are expected to be correlated with changes in temperature and BVOC emissions. These factors also have an impact on ozone production rates although their effects are smaller than those of BVOCs (Steiner et al., 2006).

Figure 3a–c show $\Delta[\text{O}_x]_{\text{chem}}/\Delta t$ for each segment (A, B, and C, respectively) vs NO_x estimated from measurements at the upwind site and in three different temperature regimes (low, medium, and high). In Fig. 3a–c, data points represent calculations of $\Delta[\text{O}_x]_{\text{chem}}/\Delta t$ for individual days, solid lines represent the mean values binned by NO_x, and the error bars are the standard error of the mean for each bin. NO_x concentrations are from observations at the upwind site, except in Fig. 3c, where Cool [NO_x] is estimated from observations at Roseville, assuming a 2 h lifetime.

We assume that NO_x observed at the upwind site is well-correlated with NO_x across the entire plume segment. For Segment A (Fig. 3a), the region between Del Paso and Roseville, $\Delta[\text{O}_x]_{\text{chem}}/\Delta t$ increases with both temperature and NO_x. The slope of $\Delta[\text{O}_x]_{\text{chem}}/\Delta t$ vs. NO_x increases as temperature increases. Figure 3b shows the behavior of $\Delta[\text{O}_x]_{\text{chem}}/\Delta t$ between Roseville and Cool (Segment B). As in Fig. 3a, O_x production rates are sensitive to both NO_x and temperature. At the low NO_x end, however, the temperature dependence is minimal. Additionally, the NO_x dependence is

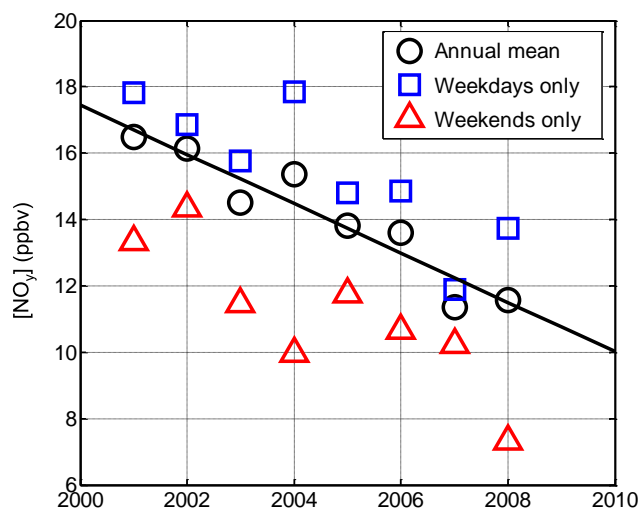


Fig. 2. Annual mean [NO_y] in the Sacramento metro region from 2001–2008. Values calculated from daily (10–1400 PST) means of 4 sites (T Street, Del Paso, Roseville, and Folsom) in each year of the study period.

a nonlinear function of NO_x with a steeper variation at lower NO_x concentrations, particularly for the medium and high temperature bins. The segment between Cool and UC-BFRS has much lower NO_x concentrations. The $\Delta[\text{O}_x]_{\text{chem}}/\Delta t$ in this segment (Fig. 3c) shows a slight increase with NO_x, but no discernable temperature dependence, except at the highest NO_x concentrations. Net O_x production rates inferred from observations are lower here than in the two upwind segments.

5 Comparison of observed ozone production with two models

The qualitative patterns of P(O_x) as a function of NO_x and temperature shown in Fig. 3a–c are consistent with predictions based on standard photochemistry. Here we make use of equations describing instantaneous O_x production derived by Murphy et al. (2006b). Briefly, O₃ participates in a null catalytic cycle with nitrogen radicals (NO and NO₂). As a result, O_x is more conserved than either individually. This so called NO_x cycle is described by Reactions (R1) to (R3).



Net O_x production occurs when some alternative oxidant facilitates the conversion of NO to NO₂. In continental regions, this is most often achieved through the oxidation of volatile organic compounds (VOCs). Reactions (R4)–(R7) outline the oxidation of VOCs by the hydroxyl radical (OH) and subsequent reaction of peroxy radicals with NO (Reactions R5

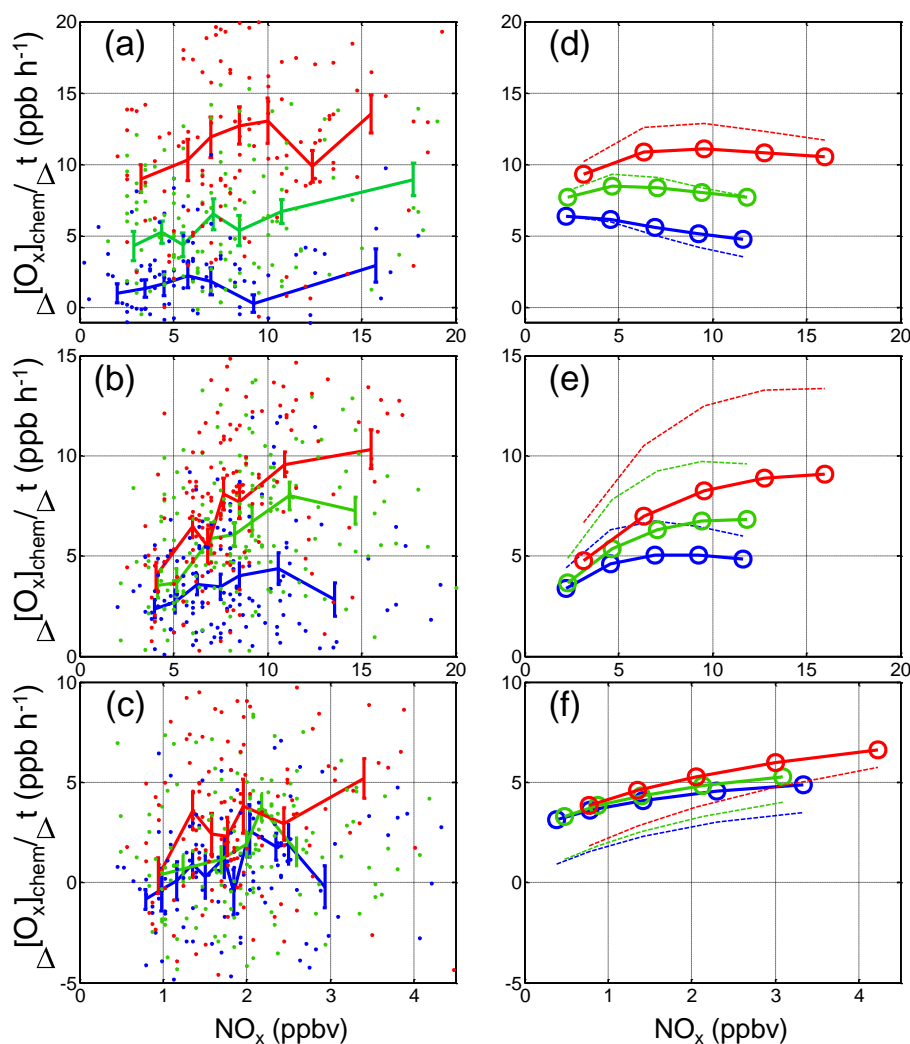
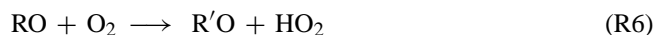
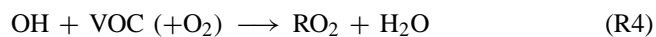


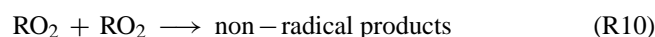
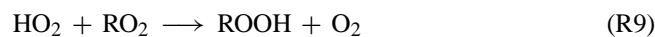
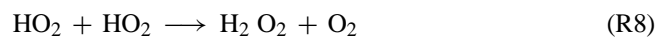
Fig. 3. Observed (a)–(c) and modeled (d)–(f) ozone production rates for three segments of Sacramento Urban Plume. Segment A, between Del Paso and Roseville, shown in (a) and (d); Segment B, between Roseville and Cool, shown in (b) and (e); Segment C, between Cool and UC-BFRS, shown in (c) and (f). In all figures, plots are color coded by temperature range: red = high, green = medium, blue = low. See Sect. 4 for additional details.

and R7), which, when coupled with NO₂ photolysis (R2 and R3), leads to net production of O₃ during the daytime. This series of reactions is radical propagating, with no net loss of NO_x or HO_x taking place. The rate of O_x production can be calculated as the combined rates of Reactions (R5) and (R7), or as approximately twice the rate of any single reaction in this cycle.



Accompanying these propagating reactions are a series of radical terminating Reactions (R8)–(R12), which ultimately

limits P(O_x) through their influence on the concentrations of the reactants in Reactions (R4)–(R7). These terminating reactions are thought of in two categories, one involving self-reactions of peroxy radicals (HO_x–HO_x, Reactions R8–R10), and one involving cross reactions between NO_x and HO_x radicals (NO_x–HO_x, Reactions R11 and R12).



Competition between these two types of radical terminating reactions is what leads to different ozone production regimes, giving rise to NO_x-limited and NO_x-suppressed or VOC-limited behavior (e.g. Sillman et al., 1990; Sillman, 1995). Non-linearities arise in the relationship between ozone production and the primary ozone precursors, NO_x and VOCs, as a result of OH suppression by NO₂ at high NO_x (Reaction R11) and peroxy radical self reactions that limit their abundance at low NO_x (Reactions R8–R10).

P(O_x) can be calculated over a range of [NO_x], VOC reactivities, and temperature by simultaneously solving steady-state equations for OH, HO₂, and RO₂ species at each input value (Kleinman et al., 1997; Thornton et al., 2002; Murphy et al., 2006b). Figure 4 shows the results from such a calculation, where P(O_x) is plotted as a function of [NO_x], and against two correlated variables: VOC reactivity ($\sum k_{4i}[\text{VOC}]_i$) on the left axis and temperature on the right axis. The VOC reactivity/temperature relationship is typical for the region, based on VOC measurements at Granite Bay (Dillon et al., 2002; Cleary et al., 2005). Direct OH reactivity measurements at UC-BFRS during BEARPEX 2007 showed similar behavior with temperature (W. H. Brune and co-workers, unpublished results). Additional reactions included in this particular calculation, not listed in the reaction series (Reactions R1–R12), are the radical propagating reactions of OH+CO and O₃+HO₂ and the photolysis of O₃ and formaldehyde. The relevant parameters for this calculation, tailored to observations in the Sacramento urban plume, are: NO₂/NO=4.5; [CO]=140 ppbv; [O₃]=53 ppbv; P(OH)=5 × 10⁶ molec cm⁻³ s⁻¹; P(HO₂)=5 × 10⁶ molec cm⁻³ s⁻¹; alkyl nitrate branching ratio ($\alpha = k_{12}/k_5$) 5 %; [M]=2.45 × 10¹⁹ molec cm⁻³. As is well known, three different photochemical regimes can be identified in these non-linear equations, a NO_x limited regime where O_x production increases with increasing NO_x and is insensitive to VOC, a NO_x suppressed or VOC limited regime where O_x production decreases with increases in NO_x and increases with increasing VOC reactivity, and a transition regime where production is relatively insensitive to changes in either parameter.

Also shown in Fig. 4 are shaded boxes representing NO_x concentrations in the Sacramento urban plume. The boxes show the range (inter-quartile) of concentrations observed in the metropolitan Sacramento region (average of 4 sites, as in Fig. 2) and the resulting concentrations in the plume after 5 hours of aging, assuming a 2 h NO_x lifetime due to the combined effects of oxidation and dilution. The boxes represent average plume conditions in the years 2001 (A and C) and 2007 (B and D) under high (red) and low (blue) temperature scenarios. To the extent that this calculation, which represents perpetual noon, can simulate the time over which O_x is produced, we interpret Fig. 4 as a prediction for the response of P(O_x) to advection and dilution of the plume. In the early years of the study period, on both weekdays and weekends and at all temperatures, the urban initialization of

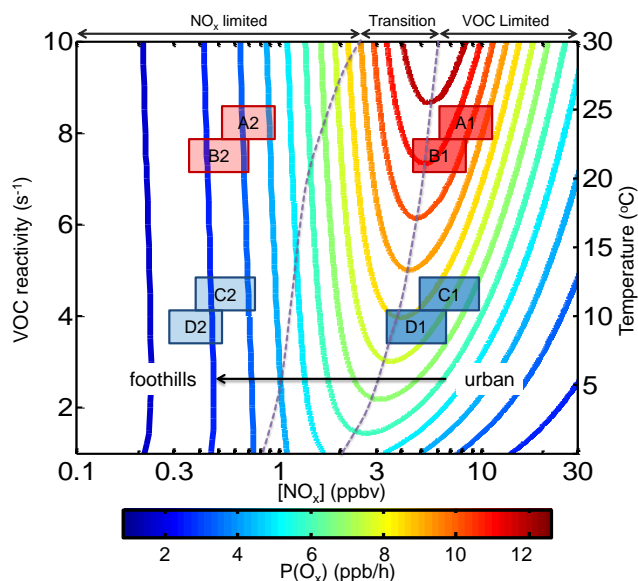


Fig. 4. Ozone production as a function of NO_x, VOC reactivity, and temperature. Contour lines represent theoretical ozone production rates over a range of NO_x and VOC reactivity phase space. See Sect. 5 for additional details.

the plume begins to the right of the ridgeline, clearly in the NO_x suppressed (VOC limited) regime. The plume always ends up well in the NO_x limited regime. By 2007, decreases in NO_x emissions have resulted in initial conditions that are essentially right at the ridgeline. The model also predicts that increases in temperature, at constant NO_x and with corresponding increases in VOC reactivity, will result in increased P(O_x) in metropolitan Sacramento and have little to no impact on P(O_x) in the foothills, as indicated by the nearly vertical contours on the left side of the figure.

We use Fig. 4 to interpret $\Delta[\text{O}_x]_{\text{chem}}/\Delta t$ as shown in Fig. 3. In the early plume evolution (Segment A) $\Delta[\text{O}_x]_{\text{chem}}/\Delta t$ increases with temperature at all NO_x values. In the low temperature range, there is not a significant trend with NO_x, while there is a clear increase with NO_x in the middle and high temperature bins. Comparing to the trends one would expect by integrating Fig. 4 during dilution (i.e. along the arrow shown), we interpret the observations as indicating that this region of the plume is NO_x limited. The data show that changes in VOC influence ozone production rates in roughly the manner expected - we observe steep increases with increasing VOC. NO_x increases result in small increases or almost no change in $\Delta[\text{O}_x]_{\text{chem}}/\Delta t$, perhaps an indication that the trajectory of the first segment moves the plume through the ridgeline, or perhaps an effect of added urban sources of VOC emissions that correlate with NO_x.

In Segment B of the plume, where it moves from Roseville to Cool, our analysis (Fig. 3b) shows an increase in P(O_x) at low NO_x and a slow increase at the highest NO_x. We interpret this slower rate of increase in P(O_x) at

high NO_x in Segment B to indicate that this segment of the plume crosses over the transition region into NO_x-limited O_x production. The temperature dependence of $\Delta[\text{O}_x]_{\text{chem}}/\Delta t$ is additional evidence that these first two segments are VOC limited. As seen in the model (Fig. 4) at fixed NO_x, O₃ production contours are a strong function of temperature. In contrast, further downwind, in Segment C, we observe an increase in $\Delta[\text{O}_x]_{\text{chem}}/\Delta t$ with NO_x that is independent of temperature indicating this segment of the plume is NO_x limited.

The qualitative interpretation of $\Delta[\text{O}_x]_{\text{obs}}/\Delta t$ as a function of temperature and NO_x is supported by this relatively simplistic photochemical model in which VOC reactivity and reaction rate constants are the only parameters that vary with temperature. In an evolving urban plume, the situation is more complex since there are accompanying factors and feedbacks that cannot be represented by a steady-state model, such as: changes in NO_x lifetime, changes in the thermal stability of peroxy nitrates, and feedbacks on primary HO_x radical production (e.g. from increased formaldehyde and O₃ in the plume). In order to provide a more quantitative analysis and demonstrate that our qualitative description of $\Delta[\text{O}_x]_{\text{chem}}/\Delta t$ as a function of temperature and NO_x is robust, we use a 1-D Lagrangian plume model that incorporates this more detailed chemistry. A brief description of the model and details particular to this work are given in Appendix A. A complete description of the model can be found in Perez (2008) and Pérez et al. (2009). This model represents diurnal variations that occur as the plume evolves along with a self-consistent representation of the chemistry and mixing.

Figure 3d–f show the results, $\Delta[\text{O}_x]_{\text{chem}}/\Delta t$ (circles with solid lines), from model calculations over a range of temperatures, with corresponding changes in BVOC emissions, and initial NO_x mixing ratios and emissions rates. $\Delta[\text{O}_x]_{\text{chem}}/\Delta t$ is calculated from the model in the same manner as from the observations – taking the O_x difference between the beginning and end points of each segment and adjusting for the effect of dilution. We also calculate the average P(O_x) over each model transect (dashed lines in Fig. 3d–f), calculated directly at each time step, using Eq. (6), and taking the segment-wide average. The qualitative similarity between P(O_x) and $\Delta[\text{O}_x]_{\text{chem}}/\Delta t$ justifies our use of $\Delta[\text{O}_x]_{\text{chem}}/\Delta t$ as an indicator of observed O_x production.

$$P(\text{O}_x) = k_2 [\text{NO}_2] - k_1 [\text{NO}] [\text{O}_3] \quad (6)$$

This model calculation, both for P(O_x) and $\Delta[\text{O}_x]_{\text{chem}}/\Delta t$, has a remarkable correspondence to the patterns in the observations. For Segment A, the model calculation shows three more or less flat and parallel lines that are well separated; for Segment B, the model calculation shows curvature that is very much like the observations; and for Segment C the model shows three curves that are almost on top of one another indicating that $\Delta[\text{O}_x]_{\text{chem}}/\Delta t$ is independent of VOC and temperature in this region a result virtually identical to the analysis of the observations.

This is not to say the correspondence is perfect. $\Delta[\text{O}_x]_{\text{chem}}/\Delta t$ in the model is too strongly NO_x suppressed in the first segment. The observations have a slightly positive slope while the model slightly negative. In Segment B, $\Delta[\text{O}_x]_{\text{chem}}/\Delta t$ does not rise as steeply as the observations or reach values as high. In Segment C, the net production at the lowest NO_x is much higher than in the observations. However, our point here is not to establish that this model is correct, but rather to establish that this method of analysis of the observations does provide a strong challenge to any model, one that is especially sensitive to O_x production chemistry.

Some of the model observation differences can be interpreted as due to the model not having the ridgeline between NO_x limited and NO_x suppressed behavior in the right location. Factors that influence the location of this the boundary and thus may contribute to the model/observation discrepancy are: (1) uncertainty in the modeled VOC reactivity, for which very few observations exist in the region; a doubling of VOC reactivity in the model increases the NO_x concentration where P(O_x) peaks by about 50 % and would result in better agreement of the model and observations, (2) uncertainty surrounding the link between isoprene oxidation products and HO_x concentrations, as indicated by recent theoretical and experimental studies (Thornton et al., 2002; Lelieveld et al., 2008; Ren et al., 2008; Hofzumahaus et al., 2009; Paulot et al., 2009; Peeters et al., 2009; Archibald et al., 2010; Da Silva et al., 2010; Stavrou et al., 2010); observations of higher oxides of nitrogen as a function of temperature by Day et al. (2008) also indicated a need for additional OH in the region. An increase in OH by a factor of 2 would increase the modeled transition point between NO_x-limited and NO_x-suppressed ozone production by 25 %, resulting in slightly better agreement between observations and the model; and (3) the uncertainty in our assumptions about the fraction of observed “NO₂” in the urban core that is true NO₂, which we estimate at 50–70 %; if NO₂ is a smaller fraction of the observed NO₂ than we estimate, the perceived transition point would occur at lower NO_x.

6 Implications for regional air quality

Regional air quality is a function of the integrated ozone production over the entire plume, P(O_x)_{tot}. From Fig. 4, an increase in temperature, and, consequently, VOC reactivity, is predicted to increase P(O_x) in the urban core, leading to an overall increase in P(O_x)_{tot} with temperature at all points in the plume, despite having little impact on P(O_x) in the NO_x-limited foothills. A reduction in NO_x emissions in the urban core, as observed in 2007 relative to 2001, may not have a significant effect on P(O_x) in the early stages of the plume or may even result in increased O₃ in the urban core, but the point of peak ozone production and then NO_x-limiting behavior will be achieved closer to the urban

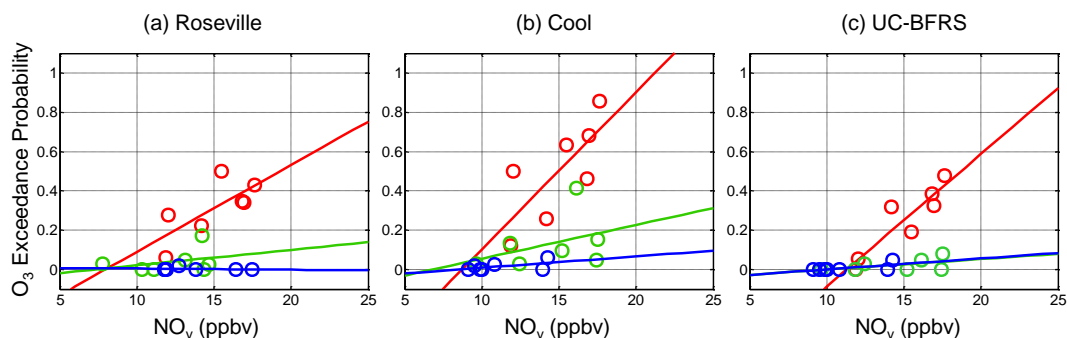


Fig. 5. O₃ exceedance probability (90 ppb 1 h standard) for hot (red), medium (green), and cold (blue) temperature days vs [NO_y]. Open circles are annual mean exceedance probabilities and [NO_y] is calculated as in Fig. 2, separated by temperature. Data shown for (a) Roseville, (b) Cool, and (c) UC-BFRS.

core and $P(O_x)_{\text{tot}}$ will decrease. This will be especially apparent at higher temperatures (higher BVOC emissions), where the $P(O_x)$ contours are a steeper function of NO_x, as illustrated in Fig. 4. Thus, it is expected that the reductions in NO_x that occurred over the period of 2001 to 2007 were more effective at reducing O₃ levels at high temperatures, where $P(O_x)$ is highest, than at low temperatures.

Our analysis of $\Delta[O_x]_{\text{chem}}/\Delta t$ above reinforces these model-based predictions for $P(O_x)$ in the Sacramento urban plume as a function of distance from the urban core, temperature, and NO_x. Comparison of these predictions of $P(O_x)$ as a function of NO_x and temperature and the probability for exceeding the 1 hour State of California ozone standard (90 ppb) on any given day during calendar years 2001–2007 provides useful insight. By focusing on the exceedance probability, variability in the annual distribution of high, medium, and low temperature days from year to year is removed, and the effects of the steady decline in NO_x emissions can be quantified. This probability is calculated for three different temperature bins and plotted against the annual region-wide average NO_y mixing ratio in Fig. 5a (Roseville), b (Cool), and c (UC-BFRS). For these probability calculations, a meteorological filter (similar to that described in Sect. 3) is used to select a subset of observation days during the ozone season. In a given year, somewhere between 60 % and 90 % of the observation days survive this filter. Table 2b summarizes the data used in these calculations. The uncertainty in the exceedance probability is calculated as $0.5(N)^{1/2}/N$, where N is the total number of days in each temperature bin for a given year. Typical uncertainties in the exceedance probability in a given year are about ± 0.1 (1σ).

A dramatic effect in the exceedance probability is observed at Cool, where, in 2001 when the annual average NO_y in the urban core was 18 ppb, nearly 70 % of the days with a maximum air temperature of at least 33 °C were over the exceedance limit; but in 2007 at an urban NO_y concentration of 12 ppb only 10 % of these days exceeded the limit (Fig. 5b). At Roseville (Fig. 5a) the sensitivity to NO_y decreases is

lower than at Cool, but still quite strong, with a 4 % decrease in the average exceedance probability for a 1 ppb decrease in NO_y. The data show a change in exceedance probability during the hot days from about 40–50 % in the early part of the study period to 10–20 % in the later part. Finally, at UC-BFRS, reductions in NO_x emissions in the Sacramento Metro region have reduced the exceedance probability at UC-BFRS, some 90 km to the northeast, from 50 % to 0 % on high temperature days (Fig. 5c). There are also reductions at lower temperatures, which are most evident at Cool.

Early in the study period, the number of exceedance days each year at UC-BFRS were comparable to that at Roseville, but the increased sensitivity to NO_x reductions in the downwind segments of the plume have resulted in a greater improvement in air quality at UC-BFRS than in the urban core and the suburbs. This effect is consistent with the differences in the day-of-week patterns of ozone in the urban core versus in the downwind regions, as outlined by Murphy et al. (2007). Nonetheless, the 30 % decrease in NO_y that occurred from 2001 to 2007 has been extremely effective in reducing the exceedance probability at all locations during the hottest days of the year when increases in biogenic emissions result in chemistry that shifts to conditions that are more NO_x limited. To put these results in perspective, if NO_y levels in 2007 had remained at 2001 levels, the 33 high temperature days during 2007 are predicted to have resulted in 22 (± 5) exceedance days at Cool, instead of the 4 that actually did occur.

It has been argued (e.g. Muller et al., 2009) that NO_x decreases cause O₃ increases in the center of cities and are more detrimental to health because of the larger number of people who live in the urban core as opposed to the surrounding suburbs and rural regions. In GSA, Murphy et al. (2007) found that O₃ concentrations (8 h maximum) increased on weekends in the urban core during the time period of 1998–2002 as a response to decreases in NO_x of approximately 20 % on weekends. We find that between 2001 and 2007, the average O₃ is higher on weekends than on weekdays only for the

Table 2b. Relaxed Filter (May–September).

Year	# Days	Wind Direction (deg.)		Wind Speed (m s ⁻¹)		[NO _y] (ppbv)		Roseville O ₃		Cool O ₃		Blodgett O ₃	
		Mean	Std. Err.	Mean	Std. Err.	Mean	Std. Err.	Exc. Days	# Days	Exc. Days	# Days	Exc. Days	# Days
<i>Hot</i>													
2001	41	236.7	1.8	3.7	0.1	16.9	1.5	14	41	28	41	13	40
2002	21	244.1	2.5	3.2	0.1	17.6	2.2	9	21	18	21	10	21
2003	26	250.7	1.5	3.2	0.1	16.8	2.1	9	26	12	26	10	26
2004	27	249.5	1.1	3.6	0.1	14.2	0.9	6	27	7	26	8	25
2005	18	245.2	2.4	2.9	0.1	12.0	1.0	5	18	9	18	1	18
2006	30	241.3	1.9	3.4	0.1	15.5	1.4	15	30	19	30	5	26
2007	33	248.7	1.3	3.4	0.1	11.9	0.9	2	33	4	32	0	11
<i>Medium</i>													
2001	39	240.1	1.7	3.6	0.1	14.7	1.4	1	39	6	37	3	37
2002	41	239.8	1.6	3.5	0.1	14.2	1.0	7	41	17	41	2	41
2003	21	242.3	1.8	3.6	0.1	14.3	2.0	0	21	1	21	0	21
2004	35	243.2	1.6	3.7	0.1	11.1	0.8	0	35	1	34	1	35
2005	21	241.9	2.1	3.3	0.1	13.1	1.7	1	21	2	21	0	18
2006	30	240.5	1.8	3.6	0.1	10.3	0.7	0	30	4	30	0	21
2007	33	242.2	1.5	3.5	0.1	7.8	0.5	1	33	1	32	0	10
<i>Cold</i>													
2001	62	234.9	1.7	3.3	0.1	16.4	1.7	0	62	0	30	0	60
2002	65	237.7	1.8	3.4	0.1	17.5	1.5	0	65	4	38	3	64
2003	50	240.8	1.7	3.3	0.1	12.7	1.6	1	50	1	30	0	47
2004	45	241.0	1.6	3.5	0.1	11.8	1.0	0	45	0	27	0	45
2005	49	239.1	1.8	3.3	0.1	11.9	1.1	0	49	0	30	0	32
2006	41	233.1	2.4	3.4	0.1	13.8	1.6	0	41	1	21	0	11
2007	60	239.0	1.4	3.3	0.1	11.8	1.0	0	57	0	31	0	11

lowest temperature days. Because O₃ concentrations on low temperature days are generally well below the exceedance limit, increases in O₃ with decreasing NO_x are not likely to lead to additional exceedances. Thus, we find no evidence that implementation of NO_x emission controls has been detrimental to air quality, by any policy-relevant metric, at any of the sites considered in this analysis over the period 2001 through 2007 (and presumably up to the present day).

We calculate a projected time frame for eliminating exceedances in the region using the data in Fig. 5 to extrapolate to a 0% exceedance probability. We calculate both a 50% confidence time-frame, from a linear fit of the mean annual exceedance probabilities and a 95% confidence time frame, from the upper bound of the 2σ uncertainty in the mean. The high temperature values at Roseville are used for these calculations. We predict, with 95% confidence, that O₃ 1-h exceedance days at all sites will be completely eliminated with a further 2/3 reduction in NO_y concentrations (and likely NO_x emissions). Assuming that the observed rate of decrease in NO_y continues, this is expected to be achieved by 2018. The 50% confidence time-frame will be reached with a 30% reduction in NO_y, which is expected to occur by 2012. This suggests that in 2012, there will be a 50% chance of no violations of the 1-h standard. This would be a first for the region since the passing of the original US Clean Air Act and regular monitoring of O₃ began in the early 1970s (CARB, 2009).

Climate change is expected to result in higher average temperatures in California, increasing biogenic VOC emissions

by 15–35% in the Sacramento region by 2050 (Steiner et al., 2006). Absent reductions in NO_x, an increase in the number of high temperature days would increase the average integrated P(O_x) in the plume and increase the probability of exceeding the 1 h O₃ standard in a given year. Between 2001 and 2007, there were on average 28 ± 7 high temperature days per year. An increase in the number of hot days would likely increase the number of exceedances; however, even a doubling of the number of annual high temperature days over the next ten years is not expected to extend the projected time frames (50% and 95%) for eliminating exceedances by more than a year. Therefore, unless there is a significant departure from the projected rate of decrease in NO_x emissions, increased high temperature days are not expected to affect the number of O₃ exceedances, in the next few decades.

An additional consideration for predicting the decline in O₃ exceedance days is the reported rise in the global tropospheric O₃ background. Parrish et al. (2009) estimate that background O_x in air transported across the Pacific has been increasing at a rate of 0.46 ppb yr⁻¹. If we increase the O₃ observed in 2007 by 5 ppb to simulate an upper limit to the effect of this increase in background O₃ after 10 years, we estimate mixing of this larger background would have the effect of increasing the frequency of violations at high temperature from 6% (in 2007) to 9% at Roseville and from 13% to 30% at Cool, with no further decrease in NO_x. However, we note that the increase reported by Parrish et al. (2009) would be largest in the recent years when NO_x is lowest. Were it

Table 2c. Strict Filter (May–September).

Year	# Days	Wind Direction (deg.)		Wind Speed (m s ⁻¹)		[NO _y] (ppbv)		Roseville O ₃		Cool O ₃		Blodgett O ₃	
		Mean	Std. Err.	Mean	Std. Err.	Mean	Std. Err.	Exc. Days	# Days	Exc. Days	# Days	Exc. Days	# Days
<i>Hot</i>													
2001	29	239.2	2.2	3.4	0.1	17.1	1.9	10	29	23	29	11	29
2002	18	244.0	2.5	3.2	0.0	18.2	2.3	8	18	15	18	8	18
2003	26	250.7	1.5	3.2	0.1	16.8	2.1	9	26	12	26	10	26
2004	24	250.3	1.1	3.5	0.1	13.9	1.1	6	24	7	24	7	22
2005	13	245.9	2.8	3.1	0.1	10.7	1.2	3	13	6	13	0	13
2006	26	242.2	1.9	3.4	0.1	16.3	1.5	13	26	17	26	5	24
2007	30	248.4	1.3	3.4	0.1	11.6	0.9	1	30	4	30	0	10
<i>Medium</i>													
2001	32	242.7	1.5	3.5	0.0	15.4	1.7	1	32	6	31	3	32
2002	37	241.4	1.5	3.4	0.0	14.0	1.1	6	37	16	37	2	37
2003	17	243.4	2.2	3.4	0.1	15.3	2.2	0	17	1	17	0	17
2004	26	245.2	1.8	3.4	0.1	11.2	1.0	0	26	1	26	1	26
2005	19	241.6	2.0	3.3	0.1	12.8	1.8	1	19	2	19	0	17
2006	23	241.9	2.0	3.4	0.1	9.4	0.8	0	23	3	23	0	16
2007	31	242.6	1.5	3.5	0.1	7.6	0.5	0	31	1	31	0	10
<i>Cold</i>													
2001	22	234.3	2.3	3.2	0.1	10.3	1.1	0	22	0	22	0	22
2002	24	240.7	2.7	3.4	0.1	12.6	1.0	0	24	4	24	1	23
2003	21	243.4	1.9	3.3	0.1	9.9	1.3	1	21	1	21	0	21
2004	19	245.3	1.9	3.4	0.1	13.2	1.5	0	19	0	19	0	19
2005	23	240.2	2.5	3.2	0.1	9.2	1.3	0	23	0	23	0	17
2006	17	239.7	2.6	3.2	0.0	11.1	1.3	0	17	1	17	0	10
2007	22	241.3	1.9	3.3	0.1	10.3	2.1	0	22	0	22	0	5

a strong effect we would expect to see a slowing of the decrease in exceedance probability at lower NO_x. We do not, a result we believe indicates growth in the background ozone has had no observable effect on the number of 1-h ozone violations in the Sacramento region.

7 Conclusions

We have presented a quantitative method for evaluating the NO_x and temperature dependence of O₃ production in an urban plume. The observational analysis represents a direct test of model chemistry. O₃ exceedance days at all points in the plume are observed to have a strong temperature dependence (Fig. 5) due to the persistence in the plume of O₃ produced in the urban core and suburbs. We show that the 30 % decrease in NO_x over the time frame of 2001 to 2007 has led to a significant decrease in O₃ 1-h exceedance days region-wide, especially during the hottest days. The reduction in exceedance days has been most significant at the farthest downwind regions of the plume. We predict that an additional decrease in NO_x will effectively eliminate O₃ 1-h exceedances in the region. At the current rate of the observed NO_y decrease (Fig. 2), we predict with 50 % confidence that exceedances will end in 2012 and with 95 % confidence that exceedances will be eliminated in the region by 2018.

Appendix A

Lagrangian urban plume model

A detailed description of the Lagrangian model of the Sacramento urban plume is given in Perez (2008) and Perez et al. (2009). The model represents mixing, photochemistry, and dry deposition as occurring in a box that is transported from Granite Bay, located close to Roseville, to UC-BFRS at a rate set by the local winds. The chemical mechanism is a reduced form of the Master Chemical Mechanism (v 3.1) with modifications as outlined in Perez et al. (2009). There are a total of 370 reactions, 170 specific chemicals, and 7 lumped species in the model.

The model is initialized with observations at Granite Bay at noon and propagated forward along the Lagrangian plume coordinates in space and time. To the east of Granite Bay anthropogenic emissions are assumed to be negligible. Biogenic VOC emissions, including isoprene, MBO, and terpenes are based on Steiner et al. (2006). Biogenic NO_x emissions are estimated from measured fluxes of soil NO_x in the oak forests of the Sierra Nevada foothills (Herman et al., 2003). At characteristic wind speeds, the plume passes over Cool after 3 hours and reaches UC-BFRS after 5 h. In order to simulate the range of conditions observed, the model is run at 3 different temperatures and 5 different initial NO_x (and NO_y) concentrations for a total of 15 separate model runs. The model inputs are variable with temperature according to

the Granite Bay observations in 2001. On top of this temperature variability, the NO_x and NO_y inputs are artificially scaled by factors of 0.33, 0.66, 1, 1.33, and 1.66 to provide 5 different NO_x scenarios for each temperature scenario.

Model outputs consist of concentrations of all species at 2 min intervals along the plume transect. The model output can be compared directly to the observations of $\Delta[\text{O}_x]_{\text{chem}}/\Delta t$ between Roseville and Cool (first 3 h of plume age) and between Cool and UC-BFRS (last 2 h of plume age). In order to simulate the segment between Del Paso and Roseville, the model is modified to start at 1000 PST, and anthropogenic emissions are simulated for the first 2 h of the transect. Equation (4) is used to calculate $\Delta[\text{O}_x]_{\text{chem}}/\Delta t$ from the model outputs in an identical manner to that used on the observations. An important advantage to using the model is that $P(\text{O}_x)$ can be calculated directly and compared to the net chemical flux of O_x as calculated by Eq. (4) in order to understand where this approach might be affected by biases when applied to the observations.

Appendix B

Entrainment of background air

For calculating $\Delta[\text{O}_x]_{\text{chem}}/\Delta t$, entrainment of background air into the plume is treated in a similar way to that described by Perez et al. (2009). A 1-D representation of the plume is used in this analysis, which is most characteristic of the center-line of the plume where mixing occurs at the top of the boundary layer with free tropospheric air. Perez et al. (2009) found that the model best reproduced observations when a low “Global” background was used, characteristic of free troposphere air. Under this scenario, a constant O₃ background of 53 ppb is assumed. The mixing rate of the plume (k_{mix}) under these conditions was calculated to be 0.31 h^{-1} .

Changes in the *absolute values* of the mixing parameters, including the entrainment rate and the O₃ background, are expected to influence the absolute values of $\Delta[\text{O}_x]_{\text{chem}}/\Delta t$, but not the observed relationships with temperature and [NO_x]. Uncertainty in the *variability* of the entrainment rate or the background concentration of O₃, however, could potentially bias our results in a way that would artificially introduce a temperature dependence to $\Delta[\text{O}_x]_{\text{chem}}/\Delta t$.

Parrish et al. (2010) found a correlative link between O₃ in background air arriving at the coast of northern California from the west and high O₃ concentrations observed in certain locations of the Central Valley 22 h later. While the role of temperature was not specifically addressed in this study, the observations of Parrish et al. (2010) imply that the relevant [O₃]_{bk} value for our analysis should be higher when temperatures are higher. Similarly, if there is a carryover effect from day to day, and [O₃]_{bk} has some dependence on the chemistry occurring in the boundary layer on the previous day in the Central Valley, it would likely be positively

correlated with temperature since warm days generally follow other warm days.

Under each of these scenarios, higher temperatures, and a corresponding higher ozone background, would lead to a slower rate of dilution for O_x in the plume and a lower inferred value for $\Delta[\text{O}_x]_{\text{chem}}/\Delta t$. To understand the potential impact of this on our results, we recalculate $\Delta[\text{O}_x]_{\text{chem}}/\Delta t$, using a temperature dependent O_x background, calculated as a linear function of temperature and normalized such that the average background over the entire 7 year period is 53 ppb with a standard deviation of 8 ppb.

This effect will have the tendency to reduce the calculated $\Delta[\text{O}_x]_{\text{chem}}/\Delta t$ at high temperatures and increase $\Delta[\text{O}_x]_{\text{chem}}/\Delta t$ at low temperatures relative to that calculated using a constant background. We find that introducing this variability to [O₃]_{bk} changes the absolute values of $\Delta[\text{O}_x]_{\text{chem}}/\Delta t$ at the high and low temperatures, but the basic features of the inferred relationship between ozone production, NO_x, and temperature are unchanged at all three segments of the transect. We find that an unreasonably large variability in [O₃]_{bk} (likely a range of 35 ppb or greater), that is perfectly correlated with temperature, would be necessary to produce the observed behavior in $\Delta[\text{O}_x]_{\text{chem}}/\Delta t$ with temperature.

Similarly, any relationship of the plume entrainment rate with temperature could give rise to a dampening of the perceived dependence of $\Delta[\text{O}_x]_{\text{chem}}/\Delta t$ on temperature. This would occur if the entrainment rate slowed with increasing temperature. A conservative upper limit for this effect was estimated previously from correlations between CO, NO_y, and temperature at UC-BFRS (Day et al., 2008); at this limit, no more than a 20 % increase in NO_y at UC-BFRS could be accounted for by a slowing of the entrainment rate with increased temperatures in the Sacramento urban plume. In our analysis, varying the entrainment rate by $\pm 20 \%$ (negatively correlated with temperature), which is more than sufficient to induce a 20 % change in NO_y at UC-BFRS, does not change the patterns of $\Delta[\text{O}_x]_{\text{chem}}/\Delta t$ with NO_x and temperature appreciably.

Appendix C

The role of anthropogenic VOCs

In our analysis we have assumed that the VOC reactivity at all points along the plume is dominated by biogenic emissions and their oxidation products. Observations at Granite Bay and UC-BFRS support this contention (Lamanna and Goldstein, 1999; Cleary et al., 2005; Steiner et al., 2008) for the suburbs and foothills. While observations of a detailed set of VOCs closer to the urban core are lacking, Steiner et al. (2008) used the CMAQ model (with a 4 km horizontal resolution) to predict about equal contributions from anthropogenic and biogenic sources to the total VOC

reactivity. From our analysis, the dependence of O₃ production on temperature suggests that the primary source of VOCs in the region, including in the urban core, have a strong temperature dependence. Presumably a major fraction of these temperature-dependent compounds are biogenics. It has been shown that evaporative anthropogenic VOC emissions can be significant in many urban locations (Rubin et al., 2006), but their contribution to the total VOC reactivity in the region is minimal compared to either the anthropogenic fuel combustion or biogenic VOC sources.

Strict regulations have resulted in a dramatic reduction of reactive VOCs in urban regions throughout California since the mid 1970s (Cox et al., 2009). According to CARB, anthropogenic VOC emissions, including those from evaporative sources, continued to decrease between 2000 and 2005 in the Sacramento Valley Air Basin at a rate of about 3% per year, similar to that reported for NO_x emissions over the same time frame (Cox et al., 2009). The likely correlation between NO_x and anthropogenic VOCs in the long-term data set begs the question: to what extent are the perceived reductions in P(O_x) with NO_x due to the accompanying changes in anthropogenic VOC emissions? This effect would be most prevalent in the region between Del Paso and Roseville, where ozone production is most sensitive to VOC concentrations and where anthropogenic VOC emissions are expected to be greatest.

The realization of NO_x reductions across two different time-scales, both interannual and day-of-week, allows us to address this question. The day-of-week changes in NO_x concentrations are thought to be primarily due to changes in the number of commercial diesel vehicles on the road from weekdays to weekends (Harley et al., 2005; Murphy et al., 2007). Since VOC emissions from diesel engines are a small fraction of total anthropogenic VOC emissions, day-of-week variability in VOC emissions are not expected to be correlated with NO_x. Conversely, over inter-annual time-scales, NO_x reductions have come primarily as a result of cleaner gasoline vehicles replacing older gasoline vehicles. VOC emissions, which are significant from gasoline vehicles, then, are expected to be correlated with NO_x emissions over the long term, but not within any given year.

Thus, a simple test of whether reductions in VOC emissions over the long term have had a significant impact on ozone production rates is to compare $\Delta[\text{O}_x]_{\text{chem}}/\Delta t$ values from the early part of the study period (2001–2002) to the later part (2006–2007) under conditions where NO_x mixing ratios and temperatures are comparable. We find that there is no significant difference in the calculated $\Delta[\text{O}_x]_{\text{chem}}/\Delta t$ values between the early period and the late period of the analysis time frame at similar temperatures and NO_x. We conclude, therefore, that there is no evidence of decreased P(O_x) between 2001 and 2007 resulting from decreases in anthropogenic VOC emissions. This comes despite a nearly equal relative decrease in VOC and NO_x emissions (Cox et al., 2009) over this time and implies that the intensity of

biogenic VOC emissions have made NO_x emission reductions more effective than anthropogenic VOC emission reductions in the region, at least downwind of Del Paso. This test also suggests that there are no additional effects correlated with the long-term fleet turn-over, such as the NO₂/NO emission ratio, that have had a detectable influence on P(O_x).

Acknowledgements. The authors thank the UC Blodgett Forest Research Station staff for logistical support, Sierra Pacific Industries for access to their land, Megan McKay for maintenance of the measurement site and data, and Rynda Hudman for helpful discussions. We would also like to acknowledge the California Air Resources Board and the California Irrigation Management System for making their data publicly available. This work was supported by the National Science Foundation (grant ATM-0639847). B. LaFranchi acknowledges support from the Camille and Henry Dreyfus Postdoctoral Program in Environmental Chemistry. A portion of this work was performed under the auspices of the US Department of Energy by Lawrence Livermore National Laboratory under Contract DE-AC52-07NA27344.

Edited by: B. Vogel

References

- Archibald, A. T., Cooke, M. C., Utembe, S. R., Shallcross, D. E., Derwent, R. G., and Jenkin, M. E.: Impacts of mechanistic changes on HO_x formation and recycling in the oxidation of isoprene, *Atmos. Chem. Phys.*, 10, 8097–8118, doi:10.5194/acp-10-8097-2010, 2010.
- Ashmore, M. R.: Assessing the future global impacts of ozone on vegetation, *Plant Cell Environ.*, 28, 949–964, 2005.
- Ban-Weiss, G. A., McLaughlin, J. P., Harley, R. A., Lunden, M. M., Kirchstetter, T. W., Kean, A. J., Strawa, A. W., Stevenson, E. D., and Kendall, G. R.: Long-term changes in emissions of nitrogen oxides and particulate matter from on-road gasoline and diesel vehicles, *Atmos. Environ.*, 42, 220–232, doi:10.1016/j.atmosenv.2007.09.049, 2008.
- Bouvier-Brown, N. C., Goldstein, A. H., Gilman, J. B., Kuster, W. C., and de Gouw, J. A.: In-situ ambient quantification of monoterpenes, sesquiterpenes, and related oxygenated compounds during BEARPEX 2007: implications for gas- and particle-phase chemistry, *Atmos. Chem. Phys.*, 9, 5505–5518, doi:10.5194/acp-9-5505-2009, 2009.
- CARB – California Air Resources Board Air Quality Database, <http://www.arb.ca.gov/aqd/aqcd/aqcd.htm>, last access: 15 September, 2009.
- Carroll, J. J., and Dixon, A. J.: Regional scale transport over complex terrain, a case study: tracing the Sacramento plume in the Sierra Nevada of California, *Atmos. Environ.*, 36, 3745–3758, 2002.
- CIMIS – California Irrigation Management Information System: <http://www.cimis.water.ca.gov/cimis/welcome.jsp>, last access: 15 September, 2009.
- Cleary, P. A., Murphy, J. G., Wooldridge, P. J., Day, D. A., Millet, D. B., McKay, M., Goldstein, A. H., and Cohen, R. C.: Observations of total alkyl nitrates within the Sacramento Urban Plume, *Atmos. Chem. Phys. Discuss.*, 5, 4801–4843, doi:10.5194/acpd-5-4801-2005, 2005.

- Cleary, P. A., Wooldridge, P. J., Millet, D. B., McKay, M., Goldstein, A. H., and Cohen, R. C.: Observations of total peroxy nitrates and aldehydes: measurement interpretation and inference of OH radical concentrations, *Atmos. Chem. Phys.*, 7, 1947–1960, doi:10.5194/acp-7-1947-2007, 2007.
- Cox, P., Delao, A., Komorniczak, A., and Weller, R.: The California Almanac of Emissions and Air Quality, California Air Resources Board, 2009.
- Da Silva, G., Graham, C., and Wang, Z. F.: Unimolecular beta-Hydroxyperoxy Radical Decomposition with OH Recycling in the Photochemical Oxidation of Isoprene, *Environ. Sci. Technol.*, 44, 250–256, doi:10.1021/es900924d, 2010.
- Day, D. A., Wooldridge, P. J., and Cohen, R. C.: Observations of the effects of temperature on atmospheric HNO₃, ΣANs, ΣPNs, and NO_x: evidence for a temperature-dependent HO_x source, *Atmos. Chem. Phys.*, 8, 1867–1879, doi:10.5194/acp-8-1867-2008, 2008.
- Day, D. A., Farmer, D. K., Goldstein, A. H., Wooldridge, P. J., Minejima, C., and Cohen, R. C.: Observations of NO_x, ΣPNs, ΣANs, and HNO₃ at a Rural Site in the California Sierra Nevada Mountains: summertime diurnal cycles, *Atmos. Chem. Phys.*, 9, 4879–4896, doi:10.5194/acp-9-4879-2009, 2009.
- Dillon, M., Lamanna, M., Schade, G., Goldstein, A., and Cohen, R.: Chemical evolution of the Sacramento urban plume: Transport and oxidation, *J. Geophys. Res.*, 107, 4046, doi:4010.1029/2001JD000969, 2002.
- Dreyfus, G. B., Schade, G. W., and Goldstein, A. H.: Observational constraints on the contribution of isoprene oxidation to ozone production on the western slope of the Sierra Nevada, California, *J. Geophys. Res.*, 107, 4365, doi:4310.1029/2001JD001490, 2002.
- Dunlea, E. J., Herndon, S. C., Nelson, D. D., Volkamer, R. M., San Martini, F., Sheehy, P. M., Zahniser, M. S., Shorter, J. H., Wormhoudt, J. C., Lamb, B. K., Allwine, E. J., Gaffney, J. S., Marley, N. A., Grutter, M., Marquez, C., Blanco, S., Cardenas, B., Retama, A., Ramos Villegas, C. R., Kolb, C. E., Molina, L. T., and Molina, M. J.: Evaluation of nitrogen dioxide chemiluminescence monitors in a polluted urban environment, *Atmos. Chem. Phys.*, 7, 2691–2704, doi:10.5194/acp-7-2691-2007, 2007.
- Farmer, D. K. and Cohen, R. C.: Observations of HNO₃, ΣAN, ΣPN and NO₂ fluxes: evidence for rapid HO_x chemistry within a pine forest canopy, *Atmos. Chem. Phys.*, 8, 3899–3917, doi:10.5194/acp-8-3899-2008, 2008.
- Feng, Z. Z. and Kobayashi, K.: Assessing the impacts of current and future concentrations of surface ozone on crop yield with meta-analysis, *Atmos. Environ.*, 43, 1510–1519, doi:10.1016/j.atmosenv.2008.11.033, 2009.
- Fuhrer, J.: Ozone risk for crops and pastures in present and future climates, *Naturwissenschaften*, 96, 173–194, doi:10.1007/s00114-008-0468-7, 2009.
- Grosjean, D. and Harrison, J.: Response of chemi-luminescence NO_x analyzers and ultraviolet ozone analyzers to organic air-pollutants, *Environ. Sci. Technol.*, 19, 862–865, 1985.
- Harley, R. A., Marr, L. C., Lehner, J. K., and Giddings, S. N.: Changes in motor vehicle emissions on diurnal to decadal time scales and effects on atmospheric composition, *Environ. Sci. Technol.*, 39, 5356–5362, 2005.
- Herman, D. J., Halverson, L. J., and Firestone, M. K.: Nitrogen dynamics in an annual grassland: oak canopy, climate, and microbial population effects, *Ecol. Appl.*, 13, 593–604, 2003.
- Hofzumahaus, A., Rohrer, F., Lu, K. D., Bohn, B., Brauers, T., Chang, C. C., Fuchs, H., Holland, F., Kita, K., Kondo, Y., Li, X., Lou, S. R., Shao, M., Zeng, L. M., Wahner, A., and Zhang, Y. H.: Amplified Trace Gas Removal in the Troposphere, *Science*, 324, 1702–1704, doi:10.1126/science.1164566, 2009.
- Kleinman, L. I., Daum, P. H., Lee, J. H., Lee, Y. N., Nunnermacker, L. J., Springston, S. R., Newman, L., WeinsteinLloyd, J., and Sillman, S.: Dependence of ozone production on NO and hydrocarbons in the troposphere, *Geophys. Res. Lett.*, 24, 2299–2302, 1997.
- Kurpius, M. R. and Goldstein, A. H.: Gas-phase chemistry dominates O₃ loss to a forest, implying a source of aerosols and hydroxyl radicals to the atmosphere, *Geophys. Res. Lett.*, 30, 1371, 2003.
- Lamanna, M. and Goldstein, A.: In situ measurements of C-2-C-10 volatile organic compounds above a Sierra Nevada ponderosa pine plantation, *J. Geophys. Res.*, 104, 21247–21262, 1999.
- Lelieveld, J., Butler, T. M., Crowley, J. N., Dillon, T. J., Fischer, H., Ganzeveld, L., Harder, H., Lawrence, M. G., Martinez, M., Taraborrelli, D., and Williams, J.: Atmospheric oxidation capacity sustained by a tropical forest, *Nature*, 452, 737–740, 2008.
- McClellan, R. O., Frampton, M. W., Koutrakis, P., McDonnell, W. F., Moolgavkar, S., North, D. W., Smith, A. E., Smith, R. L., and Utell, M. J.: Critical considerations in evaluating scientific evidence of health effects of ambient ozone: a conference report, *Inhal. Toxicol.*, 21, 1–36, doi:10.1080/08958370903176735, 2009.
- Morgan, P. B., Ainsworth, E. A., and Long, S. P.: How does elevated ozone impact soybean? A meta-analysis of photosynthesis, growth and yield, *Plant Cell Environ.*, 26, 1317–1328, 2003.
- Muller, N., Tong, D., and Mendelsohn, R.: Regulating NO_x and SO₂ Emissions in Atlanta, *B. E. J. Econ. Anal. Pol.*, 9, Art. 3, 2009.
- Murphy, J. G., Day, D. A., Cleary, P. A., Wooldridge, P. J., and Cohen, R. C.: Observations of the diurnal and seasonal trends in nitrogen oxides in the western Sierra Nevada, *Atmos. Chem. Phys.*, 6, 5321–5338, doi:10.5194/acp-6-5321-2006, 2006a.
- Murphy, J. G., Day, D. A., Cleary, P. A., Wooldridge, P. J., Millet, D. B., Goldstein, A. H., and Cohen, R. C.: The weekend effect within and downwind of Sacramento: Part 2. Observational evidence for chemical and dynamical contributions, *Atmos. Chem. Phys. Discuss.*, 6, 11971–12019, doi:10.5194/acpd-6-11971-2006, 2006b.
- Murphy, J. G., Day, D. A., Cleary, P. A., Wooldridge, P. J., Millet, D. B., Goldstein, A. H., and Cohen, R. C.: The weekend effect within and downwind of Sacramento - Part 1: Observations of ozone, nitrogen oxides, and VOC reactivity, *Atmos. Chem. Phys.*, 7, 5327–5339, doi:10.5194/acp-7-5327-2007, 2007.
- Parrish, D. D., Millet, D. B., and Goldstein, A. H.: Increasing ozone in marine boundary layer inflow at the west coasts of North America and Europe, *Atmos. Chem. Phys.*, 9, 1303–1323, doi:10.5194/acp-9-1303-2009, 2009.
- Parrish, D. D., Aikin, K. C., Oltmans, S. J., Johnson, B. J., Ives, M., and Sweeny, C.: Impact of transported background ozone inflow on summertime air quality in a California ozone exceedance area, *Atmos. Chem. Phys.*, 10, 10093–10109, doi:10.5194/acp-10-10093-2010, 2010.

- Paulot, F., Crounse, J. D., Kjaergaard, H. G., Kurten, A., St Clair, J. M., Seinfeld, J. H., and Wennberg, P. O.: Unexpected Epoxide Formation in the Gas-Phase Photooxidation of Isoprene, *Science*, 325, 730–733, 2009.
- Peeters, J., Nguyen, T. L., and Vereecken, L.: HO_x radical regeneration in the oxidation of isoprene, *Phys. Chem. Chem. Phys.*, 11, 5935–5939, doi:10.1039/b908511d, 2009.
- Perez, I. M.: The Photochemical Evolution of the Sacramento Urban Plume: a Guide to Controlling Ozone now and in a Warmer Climate, Department of Chemistry, University of California at Berkeley, Berkeley, CA, 155 pp., 2008.
- Pérez, I. M., LaFranchi, B. W., and Cohen, R. C.: Nitrogen oxide chemistry in an urban plume: investigation of the chemistry of peroxy and multifunctional organic nitrates with a Lagrangian model, *Atmos. Chem. Phys. Discuss.*, 9, 27099–27165, doi:10.5194/acpd-9-27099-2009, 2009.
- Ren, X. R., Olson, J. R., Crawford, J. H., Brune, W. H., Mao, J. Q., Long, R. B., Chen, Z., Chen, G., Avery, M. A., Sachse, G. W., Barrick, J. D., Diskin, G. S., Huey, L. G., Fried, A., Cohen, R. C., Heikes, B., Wennberg, P. O., Singh, H. B., Blake, D. R., and Shetter, R. E.: HO_x chemistry during INTEX-A 2004: Observation, model calculation, and comparison with previous studies, *J. Geophys. Res.*, 113, D05310, doi:10.1029/2007JD009166, 2008.
- Rubin, J. I., Kean, A. J., Harley, R. A., Millet, D. B., and Goldstein, A. H.: Temperature dependence of volatile organic compound evaporative emissions from motor vehicles, *J. Geophys. Res. - Atmos.*, 111, D03305, doi:10.1029/2005jd006458, 2006.
- Russell, A. R., Valin, L. C., Bucseka, E. J., Wenig, M. O., and Cohen, R. C.: Space-based Constraints on Spatial and Temporal Patterns of NO_x Emissions in California, 2005–2008, *Environ. Sci. Technol.*, 44, 3608–3615, doi:10.1021/es903451j, 2010.
- Schade, G. W., Goldstein, A. H., Gray, D. W., and Lerdau, M. T.: Canopy and leaf level 2-methyl-3-buten-2-ol fluxes from a ponderosa pine plantation, *Atmos. Environ.*, 34, 3535–3544, 2000.
- Sillman, S.: The Use of NO_y, H₂O₂, and HNO₃ as Indicators for Ozone-NO_x-Hydrocarbon Sensitivity in Urban Locations, *J. Geophys. Res.-Atmos.*, 100, 14175–14188, 1995.
- Sillman, S., Logan, J. A., and Wofsy, S. C.: The Sensitivity of Ozone to Nitrogen-Oxides and Hydrocarbons in Regional Ozone Episodes, *J. Geophys. Res.-Atmos.*, 95, 1837–1851, 1990.
- Spaulding, R. S., Schade, G. W., Goldstein, A. H., and Charles, M. J.: Characterization of secondary atmospheric photooxidation products: Evidence for biogenic and anthropogenic sources, *J. Geophys. Res.*, 108, 4247, doi:10.1029/2002JD002478, 2003.
- Stavrakou, T., Peeters, J., and Müller, J.-F.: Improved global modelling of HO_x recycling in isoprene oxidation: evaluation against the GABRIEL and INTEX-A aircraft campaign measurements, *Atmos. Chem. Phys.*, 10, 9863–9878, doi:10.5194/acp-10-9863-2010, 2010.
- Steinbacher, M., Zellweger, C., Schwarzenbach, B., Bugmann, S., Buchmann, B., Ordóñez, C., Prevot, A. S. H., and Hueglin, C.: Nitrogen oxide measurements at rural sites in Switzerland: Bias of conventional measurement techniques, *J. Geophys. Res.-Atmos.*, 112, D11307, doi:10.1029/2006jd007971, 2007.
- Steiner, A. L., Tonse, S., Cohen, R. C., Goldstein, A. H., and Harley, R. A.: Influence of future climate and emissions on regional air quality in California, *J. Geophys. Res.*, 111, D18303, doi:10.1029/2005JD006935, 2006.
- Steiner, A. L., Cohen, R. C., Harley, R. A., Tonse, S., Millet, D. B., Schade, G. W., and Goldstein, A. H.: VOC reactivity in central California: comparing an air quality model to ground-based measurements, *Atmos. Chem. Phys.*, 8, 351–368, doi:10.5194/acp-8-351-2008, 2008.
- Tang, G., Li, X., Wang, Y., Xin, J., and Ren, X.: Surface ozone trend details and interpretations in Beijing, 2001–2006, *Atmos. Chem. Phys.*, 9, 8813–8823, doi:10.5194/acp-9-8813-2009, 2009.
- Thornton, J., Wooldridge, P., and Cohen, R.: Atmospheric NO₂: In situ laser-induced fluorescence detection at parts per trillion mixing ratios, *Anal. Chem.*, 72, 528–539, 2000.
- Thornton, J. A., Wooldridge, P. J., Cohen, R. C., Martinez, M., Harder, H., Brune, W. H., Williams, E. J., Roberts, J. M., Fehsenfeld, F. C., Hall, S. R., Shetter, R. E., Wert, B. P., and Fried, A.: Ozone production rates as a function of NO_x abundances and HO_x production rates in the Nashville urban plume, *J. Geophys. Res.*, 107, 4146, doi:10.1029/2001JD000932, 2002.
- Trasande, L. and Thurston, G. D.: The role of air pollution in asthma and other pediatric morbidities, *J. Allergy Clin. Immun.*, 115, 689–699, doi:10.1016/j.jaci.2005.01.056, 2005.
- Uysal, N. and Schapira, R. M.: Effects of ozone on lung function and lung diseases, *Curr. Opin. Pulm. Med.*, 9, 144–150, 2003.
- Winer, A. M., Peters, J. W., Smith, J. P., and Pitts, J. N.: Response of commercial chemiluminescent NO-NO₂ analyzers to other nitrogen-containing compounds, *Environ. Sci. Technol.*, 8, 1118–1121, 1974.
- Yang, W. and Omaye, S. T.: Air pollutants, oxidative stress and human health, *Mutat. Res.-Gen. Tox. En.*, 674, 45–54, doi:10.1016/j.mrgentox.2008.10.005, 2009.
- Zavala, M., Lei, W., Molina, M. J., and Molina, L. T.: Modeled and observed ozone sensitivity to mobile-source emissions in Mexico City, *Atmos. Chem. Phys.*, 9, 39–55, doi:10.5194/acp-9-39-2009, 2009.